Structure and Spectroscopy of Surface Defects from Scanning Force Microscopy: Theoretical Predictions

Lev N. Kantorovich, Alexander L. Shluger, and A. Marshall Stoneham

Department of Physics and Astronomy, University College London,
Gower Street, London WC1E 6BT, United Kingdom
(Received 5 June 2000)

A possibility to study surface defects by combining noncontact scanning force microscopy (SFM) imaging with atomically resolved optical spectroscopy is demonstrated by modeling an impurity Cr^{3+} ion at the MgO(001) surface with a SFM tip. Using a combination of the atomistic simulation and the *ab initio* electronic structure calculations, we predict a topographic noncontact SFM image of the defect and show that its optical transitions can be either enhanced or suppressed depending on the tip atomistic structure and its position relative to the defect. These effects should allow identification of certain impurity species through competition between radiative and nonradiative transitions.

Scanning force microscopy (SFM) promised characterization of the structure and properties of *individual* surface defects and chemically active sites. Such surface defects, impurities, adsorbed species, and low-coordinated surface sites are critical in catalysis, chemical sensing, film growth, photo- and electrochemical reactions, and other surface processes. These surface defects proved to be notoriously difficult to identify. There are several reasons. The first is insufficient SFM resolution, although this is constantly improving. Low defect concentrations and high defect mobility are serious obstacles. The most serious problem is the inability of SFM alone to determine reliably the chemical identity of defect species. True atomic resolution on semiconductors and insulators has been obtained using noncontact (NC)-SFM [1–4], yet the nature of most defects seen with NC-SFM has still to be established.

Our aim is to seek ways to establish the identity of observed individual defects and study their properties. How can one tell defect A from defect B? Topographic SFM images help if there is a reliable theoretical "portrait" of each defect for comparison. Unambiguous identification needs more information. Moreover, for typical concentrations and typical scanning areas (50×50 Å), one is unlikely to encounter more than one defect of each kind. Measuring optical absorption usually only confirms the presence of a certain defect within the sample. To identify a *particular* defect, one must correlate topographic and, say, spectroscopic signals, perhaps by perturbing defect excited states by the SFM tip. Specifically, the SFM probe can alter the balance between radiative and nonradiative defect processes. In this Letter, we use state-of-the-art theory to show how one might monitor the change in yield and/or excitation energy of luminescence as a function of tip position. We show that the SFM tip can alter the spectroscopic properties of an ion significantly. A combination of atomically resolved force and SFM-modulated optical spectroscopies appears promising for surface defect studies. Further, the effects we shall describe are sensitive to the host surface dipole, and some estimate of surface rumpling can be obtained from this dipole, as well as from information in the image.

We shall evaluate the feasibility of our approach for the Cr^{3+} ion in MgO. We treat this as a prototype system which is relatively easy to calculate. This impurity has been studied both experimentally [5,6] and theoretically [7] in the bulk of MgO. The Cr^{3+} ion substitutes for Mg. In the $[Ar]d^3$ electronic configuration, the three d electrons are well localized by a strong crystal field. The net defect charge is compensated by cation vacancies (one vacancy for every two Cr^{3+} ions), which need not be close to the impurity [5,6]. Chromium ions are found with several symmetries: cubic (which we discuss), tetragonal, and orthorhombic. The cubic-site ions are in abundance and are responsible for a broad 2.00 eV *absorption* band and 1.96 eV *luminescence* band [5,6]. These bands are attributed to transitions between the ground ^4A and excited ^4T states which are parity forbidden, and become allowed only through electron-lattice coupling or applied electric fields. Low-symmetry chromium sites give further features in the absorption and luminescence spectra; we shall not discuss these.

The spectra depend strongly on the local symmetry, even in the bulk. This suggests that there should be even more pronounced effects at the surface, and that such effects might be controlled by interaction with the SFM tip. We confirm this by calculating both a topographic NC-SFM image of Cr^{3+} ion at the MgO(001) surface and its optical properties (energy, oscillator strength) as a function of the SFM tip position.

Ionic crystals have proved difficult to study with SFM. There have been successful attempts to image thin insulating films grown on metal substrates [8,9]. Thin films do not have charging problems, and their chemical composition can be controlled more easily. We model the more general film case (Fig. 1); however, most of our results are equally applicable to crystalline samples. The conductive
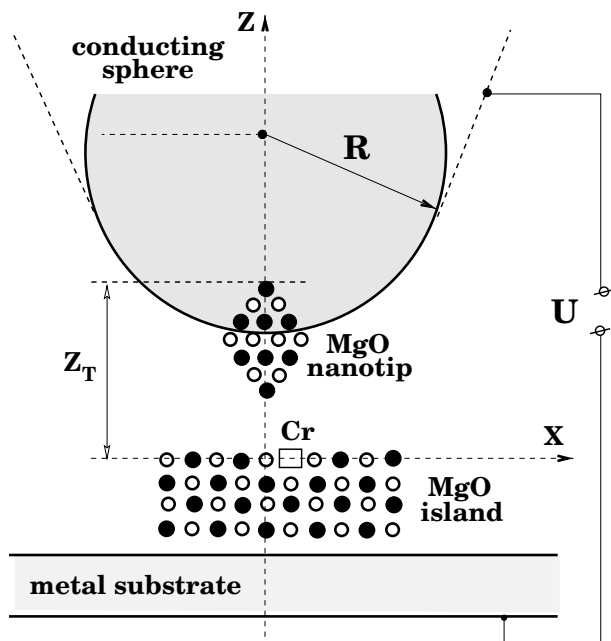
FIG. 1. Schematic of the SFM model used to simulate the interaction between the tip and the sample.

substrate is covered by an insulating film; there are oxide islands (nanoclusters) on the conductive tip surface. A voltage, U, is applied between tip and substrate. The tip has conical shape with a sphere of radius R at the apex.

NC-SFM employs frequency modulation, with the cantilever driven at its resonant frequency at constant oscillation amplitude [10]. Contrast formation in NC-SFM on cubic ionic surfaces is discussed in detail in Ref. [11]. In our calculations the resonance frequency was $f_0 = 158.3$ kHz and the amplitude 36 Å. We model the topographic mode, in which a feedback loop displaces the sample to maintain a constant frequency shift caused by the tip-sample interaction. The z displacements of the sample during scanning, averaged over many cantilever oscillations, yield a topographic image of the surface.

First, we calculate the force field of the tip-surface interaction [11]. The end of the tip is represented by a conducting sphere of radius 100 Å with a 64-atom MgO nanocluster cube embedded at the apex (see Fig. 1). As regards the electric field and electric field gradient due to the tip, this is a good *model* of real oxidized Si tips [12]. The nanocluster is oriented to have its ⟨111⟩ axis perpendicular to the surface, and terminates in either a single oxygen or a single magnesium ion. The MgO film on the substrate is simulated by the five-layer 9×9 island. The forces between the tip and sample include (i) the long-range van der Waals force between the macroscopic part of the tip and the substrate, (ii) the image force due to polarization of the conducting tip and the substrate by the tip oxide and the ionic insulating film, and (iii) short-range and Coulomb forces between the oxide nanocluster on the tip and the MgO film calculated using a shell model. The

model is very similar to that used in our recent work on the SFM imaging of NaCl film grown on Cu [9]. Our present work goes further by including image forces on ions self-consistently [13,14]. Non-Coulomb interactions between the ions are simulated by Buckingham two-body potentials [15]. Both tip and surface ions were allowed to relax at each tip position. In characterizing the tip-surface separation, we refer to the distance Z_T between the frozen ion at the top of the MgO cube (which is inside the sphere) and the ideal surface plane (see Fig. 1). Subtracting 10 Å from Z_T one should have an estimate of a distance between the atom at the tip end and the surface plane. Full details are given in Ref. [16].

The force field $F_{\text{tip}}(X_T, Y_T, Z_T)$ is calculated on a mesh of lateral positions X_T, Y_T of the tip above the film and on a grid of Z_T values from 12.5 to 100 Å. The tip oscillations are large in amplitude, making large separations necessary. The calculated 3D image of the Cr^{3+} ion in the top surface layer at the frequency shift of 235 Hz is shown in Fig. 2. If we choose a nanotip terminated by an Mg cation, we find that peaks in the perfect part of the lattice correspond to the surface O ions; the minima correspond either to surface Mg ions or to midway positions between the surface oxygens. The defect has a well-defined image in which the Cr site itself is not well resolved. The lack of resolution results from the significant lattice distortion around the Cr^{3+} ion: the four in-plane oxygens displace by 0.27 Å towards the Cr ion and by 0.12 Å downwards (which are 12.7% and 5.6% of the Mg-O distance in the perfect lattice, respectively). In turn, the Cr ion moves downwards from its ideal site by 0.26 Å (12.3%) and the O ion underneath is displaced upwards by 0.04 Å (1.9%). At large distances ($Z_T \geq 13.5$ Å), the complex of the Cr ion and surrounding oxygens is seen as a whole, and is more attractive than a perfect O site. It becomes less attractive at closer approach, and, for $\Delta f = 235$ Hz, the Mg
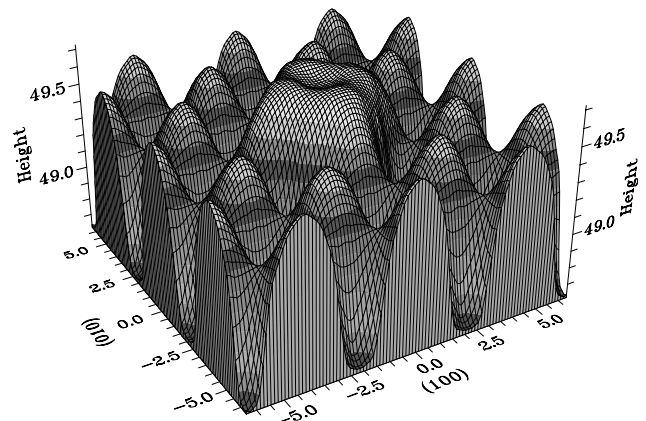

FIG. 2. The simulated NC-SFM image of the Cr^{3+} defect at the MgO (001) surface for the frequency shift $\Delta f = 235$ Hz. The image corresponds to the z displacement of the sample, Z_T, with respect to the *equilibrium* position of the cantilever (in Å). Note that the oscillation amplitude is 36 Å.

terminated tip can sense the repulsion of the Cr ion. If we chose an oxide nanocluster terminating in an O anion, the image is reversed.

We now turn to the effect of the tip on the spectroscopic properties of the Cr ion. We use an embedded cluster method, similar to that of Ref. [17]. The Cr ion is situated at the center of the top layer of a cluster of $9 \times 9 \times 5$ point ions. The positions of cluster ions with and without the tip were determined using classical pair potentials, as described above. However, the Cr ion and five nearest neighbor oxygens were treated quantum mechanically. Each oxygen ion, in turn, was surrounded by the nearest shell of magnesium ions treated as bare pseudopotentials [18]. Altogether, the quantum cluster included 19 atoms in the case of the surface Cr defect. The matrix elements of electrostatic potential due to all other classical ions in the MgO cluster are included in the Hamiltonian as point charges, using the method implemented in GAUSSIAN94 [19]. Further, we include the electrostatic potential produced by the image charges due to polarization of the conductive tip and substrate by the tip oxide and by the MgO film in the electronic structure calculations.

All electrons on the oxygen ions were included in the calculations, using the standard 6-31G basis set. The optical excitation and luminescence energies were calculated using a complete active space self-consistent field (CASSCF) method [20], which treats the wave function of both the ground and excited defect states as a linear combination of determinants. To make the study of the tip effect feasible, we treated only the d electrons on Cr explicitly using a "large core" pseudopotential. The basis set on the Cr ion included $3d$ and $4p$ orbitals, and was optimized using the full-electron CASSCF calculations of a free ion to reproduce the experimental optical transition energies. The calculated $^4F \rightarrow {}^4P$ and $^4F \rightarrow {}^2G$ transition energies are equal to 1.9 and 2.0 eV, in reasonable agreement with 1.71 and 1.82, respectively, for a free ion. The $^4A \rightarrow {}^4T$ optical transition in the MgO bulk is almost completely confined to d states, and has zero oscillator strength. The lower symmetry at the surface splits the triply degenerate Cr excited state ^4T into singly and doubly degenerate (E) states, which include some admixture of $4p$ states. The energy of the $^4A \rightarrow {}^4E$ transition of the Cr ion at the surface in our cluster model is 1.85 eV, with nonzero oscillator strength.

We now examine the effect of the tip on the optical transitions of the surface Cr ion in the constant height mode [3]. First consider a tip like that used for the topographic image, with an ionic MgO nanocrystalline island on a conductive tip of apex radius $R = 100$ Å (Fig. 1). In our calculations, we assume a potential difference of 1 V between the conductive tip and the substrate. The low-coordination corner of the MgO cube nearest to the surface produces a strong, inhomogeneous, electric field over an area of atomic dimensions. This is characteristic for other oxide tips as well as a Si tip with adsorbed oxygen or polar species [12]. This field can affect the electric dipole

transition of the impurity strongly. Whether the nanocluster terminates in an Mg or O ion can determine the sign of some effects.

The tip atomic structure has a strong effect on the optical transition probability of the defect. The Mg-terminated tip gives rise to a field which enhances the level splitting and the admixture of $4p$ states in the excited state, thus increasing the intensity by more than 30%. An O-terminated tip essentially recreates the bulk Cr coordination, and so suppresses the transition completely by reducing the transition matrix element. Since the electron excitation is between two highly localized d states, the transition energy change does not exceed 0.05 eV. Figure 3 shows the relative oscillator strength (with respect to that calculated for infinite separation) of the $^4A \rightarrow {}^4E$ transition as a function of tip position as the tip scans parallel to the surface at the height about 3 Å from the ideal surface plane. One can see that the tip has pronounced effect only when very close to the Cr ion.

Analysis of the electron density in the excited state shows that (for O or Mg termination) it is still strongly localized on the Cr ion, so we do not expect significant change in the topographic image of the defect in the excited state. Further, the small change in charge density upon excitation suggests that Stokes shift of the luminescence should be small. The same conclusion is supported by our calculations of the adiabatic potential of the excited state along several configuration coordinates, described in Ref. [16]. Therefore, we believe that the effect of the tip on the luminescence energy and transition matrix element should be very similar to that on the optical excitation.

The transitions we have considered would have zero oscillator strength in the bulk. At the surface, there is an electric field in the absence of the tip, and so a finite oscillator strength. The field produced by the tip is primarily due to its *atomic structure*. A conductive tip consisting of
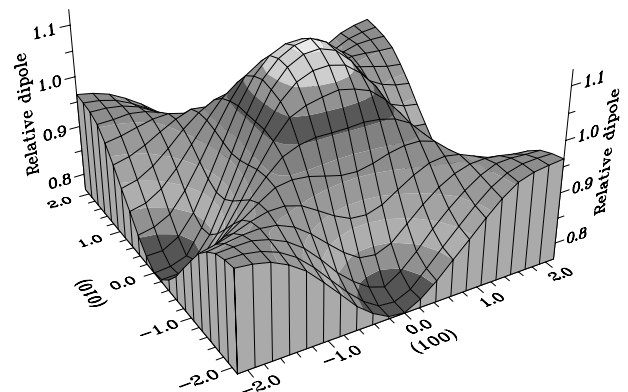

FIG. 3. The 3D plot of the relative oscillator strength calculated for the constant tip height of $Z_T = 13$ Å (about 3 Å above the surface). The Cr ion is in the center of the region comprising four adjacent unit cells. The excited ^4E state is split into two for the off-center position of the Mg-terminated tip, and we show the transition into one of the two states.

just a few atoms could give similar electric fields and field gradients to our model tip. A conductive tip of apex radius R greater than 10 Å but without the oxide nanocluster produces an almost homogeneous electric field in the quantum cluster and shows very modest effects of voltage and the tip position on the transition properties. However, with the oxide present, even a modest dependence on applied voltage U will give an opportunity to gain more information about tip or defect. Thus (i) we might characterize a tip using a standard defect, perhaps MgO:Cr, for use in quantitative analysis of other defects, (ii) we may be able to estimate the effective electric field at the Cr in the absence of the tip (that would depend on whether or not we could detect any U dependence), and (iii) the presence of the tip fields modifies the radiative/nonradiative transition branching ratio, and we should be able to gain information about the nonradiative processes as a function of temperature.

To summarize, our calculations predict a characteristic topographic image of the Cr^{3+} impurity center in NC-SFM and a pronounced effect of the SFM tip on its optical properties. The two effects can be correlated, e.g., through observation of an enhanced luminescence signal and energy shift when the tip is probing the defect center. This result only weakly depends on the film thickness although some small changes could be expected for thinner (less than five layers) films. The predicted effect would be even stronger for excited defect states which are less localized than these of the Cr ion considered here. In systems with excited state lifetimes exceeding the tip oscillation period, changes in the topographic image with electronic state could be observed.

We regard this work as a theoretical demonstration of the possibility to study individual defects combining force imaging with spectroscopy. Experimental techniques necessary for the experiment we suggest are being developed in the area of scanning near-field optical microscopy (SNOM) [21,22]. SFM/SNOM aperture probes fabricated using conventional optically transparent SFM tips allow one to obtain topographic images and *simultaneously* excite surface nanoscale species and collect luminescence in near field [23,24]. Very small specially shaped apertures already in use (200 Å across which is several times smaller than a typical distance for most impurities) should allow one to get an optical signal from isolated defects; very weak optical signals can be collected by photon counting [25]. Efforts are made to fabricate SFM/SNOM tips capable of providing atomic resolution in topographic SFM images [24]. Therefore, we believe the approach suggested in this work will help defect identification and may open new avenues for investigating properties of individual species at surfaces.

[1] *Proceedings of NC-AFM 98* [Appl. Surf. Sci. **140** (1999)]; *Proceedings of NC-AFM 99* [Appl. Surf. Sci. **157** (2000)].
[2] *Proceedings of SXM-3* [Surf. Interface Anal. **27** (1999)].
[3] M. A. Lantz *et al.,* Phys. Rev. Lett. **84**, 2642 (2000).
[4] A. Schwarz, W. Allers, U. D. Schwarz, and R. Wiesendanger, Phys. Rev. B **61**, 2837 (2000).
[5] B. Henderson and G. F. Imbusch, *Optical Spectroscopy of Inorganic Solids* (Clarendon Press, Oxford, 1989).
[6] M. B. O'Neill and B. Henderson, J. Lumin. **39**, 161 (1988).
[7] D. J. Groh, R. Pandey, and J. M. Recio, Radiat. Eff. Defects Solids **134**, 127 (1995).
[8] R. Bennewitz, M. Bammerlin, M. Guggisberg, C. Loppacqher, A. Baratoff, E. Meyer, and H.-J. Güntherodt, Surf. Interface Anal. **27**, 462 (1999).
[9] R. Bennewitz *et al.,* Phys. Rev. B **62**, 2074 (2000).
[10] F. J. Giessibl, Science **267**, 68 (1995).
[11] A. I. Livshits, A. L. Shluger, A. L. Rohl, and A. S. Foster, Phys. Rev. B **59**, 2436 (1999).
[12] P. V. Sushko, A. S. Foster, L. N. Kantorovich, and A. L. Shluger, Appl. Surf. Sci. **144-145**, 608 (1999).
[13] L. N. Kantorovich, A. I. Livshits, and A. M. Stoneham, J. Phys. Condens. Matter **12**, 795 (2000).
[14] L. N. Kantorovich, A. Foster, A. L. Shluger, and A. M. Stoneham, Surf. Sci. **445**, 283 (2000).
[15] R. W. Grimes, C. R. A. Catlow, and A. M. Stoneham, J. Phys. Condens. Matter **1**, 7367 (1989).
[16] L. N. Kantorovich, A. L. Shluger, and A. M. Stoneham (to be published).
[17] A. L. Shluger, P. V. Sushko, and L. N. Kantorovich, Phys. Rev. B **59**, 2417 (1999).
[18] W. R. Wadt and P. J. Hay, J. Chem. Phys. **82**, 284 (1985).
[19] M. J. Frisch *et al., Gaussian94, Revision D.1* (Gaussian, Inc., Pittsburgh, PA, 1995).
[20] N. Yamamoto, T. Vreven, M. A. Robb, M. J. Frisch, and J. B. Schlegel, Chem. Phys. Lett. **250**, 373 (1996).
[21] S. Nishikawa and T. Isu, J. Microsc. **194**, 415 (1999).
[22] A. Richter, M. Süptitz, Ch. Lienau, T. Elsaesser, M. Ramsteiner, R. Nötzel, and K. H. Ploog, J. Microsc. **194**, 393 (1999).
[23] H. Zhou, A. Midha, G. Mills, L. Donaldson, and J. M. R. Weaver, Appl. Phys. Lett. **75**, 1824 (1999).
[24] D. Drews, W. Ehrfeld, M. Lacher, K. Mayr, W. Noell, S. Schmitt, and M. Abraham, Nanotechnology **10**, 61 (1999).
[25] H. Zhou, B. K. Chong, P. Stopford, G. Mills, A. Midha, L. Donaldson, and J. M. R. Weaver (private communication).